SMALL-AVALANCHE EXPERIMENTS IN NISEKO, JAPAN: TRIALS AND RESULTS 2016−2025

Yoichi Ito[1]*, Kouichi Nishimura[2,3], Satoru Yamaguchi[1], Yoshihiko Saito[3], Hirofumi Niiya[4], Sojiro Sunako[1], Kae Tsunematsu[5], Ryo Honda[6], Shinichiro Horikawa[7], Koji Fujita[7], Tsubasa Okaze[8], Cristina Pérez-Guillén[9], Dieter Issler[10], Piotr Kupiszewski[10], Jan-Thomas Fischer[11], Marc Adams[11], Anselm Köhler[11], Shoichi Mori[12], Kazuyuki Fujita[12], and Akio Shinya[13]

[1] *Snow and Ice Research Center, National Research Institute for Earth Science and Disaster Resilience (NIED), Japan*
[2] *Professor Emeritus of Nagoya University, Japan*
[3] *Yukiken Snow Eaters Co. Ltd., Japan*
[4] *Research Institute for Natural Hazards and Disaster Recovery, Niigata University, Japan*
[5] *Faculty of Science, Yamagata University, Japan*
[6] *Mount Fuji Research Institute, Japan*
[7] *Graduate School of Environmental Studies, Nagoya University, Japan*
[8] *School of Environment and Society, Institute of Science Tokyo, Japan*
[9] *WSL Institute for Snow and Avalanche Research SLF, Switzerland*
[10] *Norwegian Geotechnical Institute (NGI), Norway*
[11] *Austrian Research Centre for Forests (BFW), Austria*
[12] *Institute of Low Temperature Science, Hokkaido University, Japan*
[13] *Niseko Avalanche Institute, Japan*

ABSTRACT: Small-avalanche experiments were conducted in the Niseko-Annupuri mountain range in Japan from 2016 to 2019 and in 2025 to obtain small avalanche dynamics data. In the experiments small avalanches were triggered using blasting or a snow groomer by pushing and collapsing piled-up snow. The avalanches ranged in runout distance approximately from 30 to 200 meters. Avalanche velocity was estimated from aerial drone footage; additionally, Doppler radar provided reliable data even for the small-scale event. Internal velocity was also obtained by releasing sensors containing IMU and GNSS units within the avalanche flow. The flow behavior of the avalanches was observed using the infrared camera and by surveying debris; however, no significant variations were observed due to the short runout distance. We also carried out seismic and infrasound monitoring, however, no significant variations in the infrasound waveforms were detected.

KEYWORDS: small avalanche, avalanche experiment, sensor

1. INTRODUCTION

Small avalanches frequently occur in Japan during the winter season, typically from road-side slopes, leading to cumulative social damage by blocking transport networks and supply chains. Following these small avalanches, efforts are usually concentrated on clearing the debris and restoring traffic, and detailed observations are rarely carried out. Conversely, when large-scale avalanches occur, even if the damage itself is minor, their formation and dynamic processes are often investigated and documented in detail. Consequently, a gap arises; our understanding of small avalanches, which occur relatively frequently and in close locations, remains poorly understood.

There is a similar gap in avalanche research. Over many years, significant data has been accumulated at large-scale avalanche test sites with slopes extending over several kilometers, such as the Vallée de la Sionne in Switzerland (Sovilla et al., 2013) and Ryggfonn in Norway (Gauer and Kristensen, 2016). On the other hand, small-avalanche experiments (SAEs) have also been conducted in the past in the United States (Dent et al., 1998), Italy (Sommavilla and Sovilla, 1998; Barbero et al., 2013; Maggioni et al., 2019), and China (Abe et al., 1999), with data on velocity, impact pressure, and other parameters, having been reported. However, these have generally been one-off experiments exploring only a small sample of possible avalanche behavior, and the volume of data acquired is very small compared to that for large-scale avalanches. Consequently, when validating avalanche dynamics models, for example, the models are typically tuned using data from a large number of large-scale avalanche events and experiments (e.g. Christen et al., 2010). In the case of small avalanches, the single (or few) measurement(s) may not represent the behaviour of rare events, which typically are the decisive ones in hazard mapping and dimensioning of mitigation measures, and may thus lead to inadequate calibration of numerical models (Maggioni et al., 2012).

* Corresponding author address:
Yoichi Ito, Snow and Ice Research Center, National Research Institute for Earth Science and Disaster Resilience, Nagaoka 940-0821, Japan;
tel: +81 258-35-7520; fax: +81 258-35-0020
email: y_ito@bosai.go.jp

https://doi.org/10.15788/1790098800

One possible approach, in some respects comparable to SAEs, is to conduct experiments in large chutes by releasing large amounts of snow (e.g. Kern et al., 2004; Vilajosana et al., 2011; Schaefer, 2016). This is useful for understanding the fundamental dynamics and internal structure of avalanches, as it allows for repeated testing of conditions that are difficult to replicate in real mountain slopes. However, it is insufficient for fully validating two- or three-dimensional dynamics models.

Therefore, we carried out SAEs in Japan from 2016 with the aim of collecting data on avalanche dynamics. Due to strict restrictions on the use of explosives in Japan, no artificial avalanche experiments using explosives had been carried out since the 1980s. In recent years, however, explosives have been increasingly used to secure exposed ski runs. We therefore collaborated with a ski resort employing avalanche control operations to conduct SAEs. Furthermore, to examine whether avalanche experiments could be carried out without the use of explosives, we also tested a method of triggering avalanches using snow groomers. Here, we present the results of experiments conducted during the winter seasons of 2016−19 and 2025; supplementing the previously reported initial findings in Nishimura et al. (2018), and discuss the future prospects for SAEs.

2. EXPERIMENTAL SITES AND INSTRUMENTATION

Snow avalanche experiments were conducted in the vicinity of the ski resort on Mt. Niseko-Annupuri (1308 m a.s.l.) in Hokkaido, Japan (Fig. 1). The experimental sites can be divided into two main areas. One was Mizuno-no-Sawa within the Niseko Village Ski Resort, a backcountry zone that is opened to the public following avalanche control operations using explosives (Figs. 2a and 2c). After skiing had been prohibited due to the widespread formation of cracks in March, ski patrols triggered an avalanche using explosives for the experiment. In 2025, an attempt was also made to observe avalanches occurring during avalanche control operations in mid-winter. Another experimental site was the Moiwa Bowl, a backcountry zone near the Niseko Moiwa Ski Resort (Fig. 2b). Here, a method using a snow groomer was employed to trigger a small avalanche by pushing piled-up snow. While this method has a lower probability of triggering avalanches compared to methods using explosives, it has the advantage of allowing observations to be carried out relatively safely.

The experiments began in 2016 under a five-year project. They continued until 2019, but the project

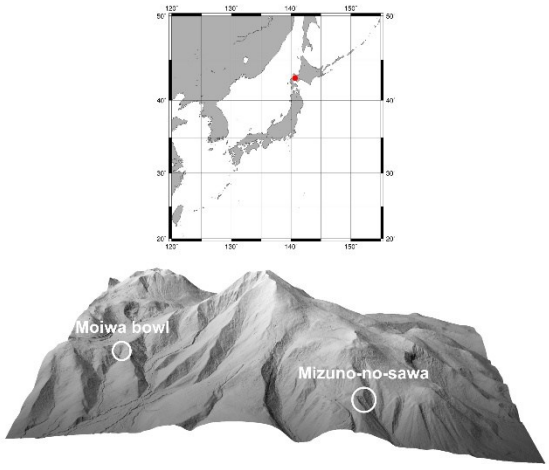


Figure 1: Location of Mt. Niseku-Annupuri in Japan (top, red dot in figure) and the experimental slopes, Mizuno-no-sawa and Moiwa Bowl in Mt. Niseku-Annupuri (bottom).

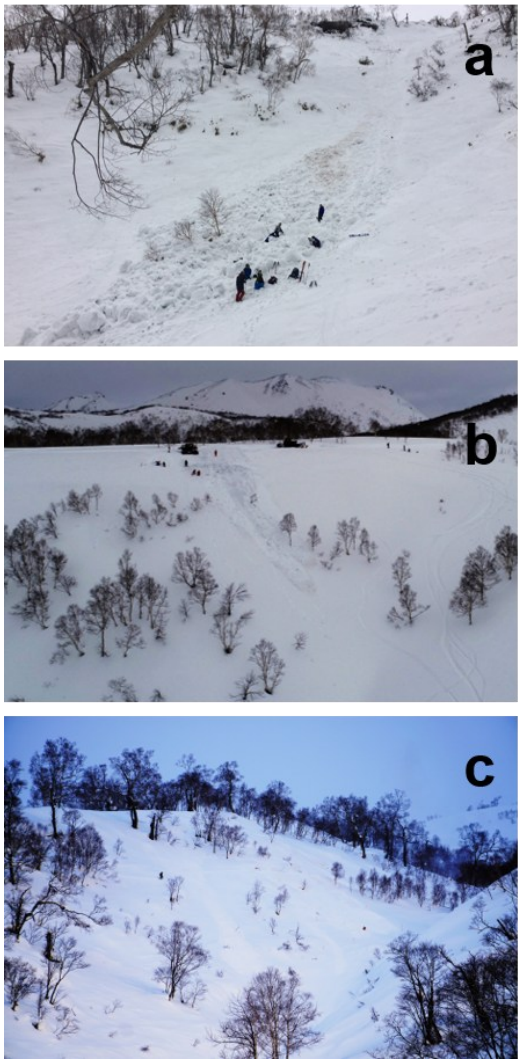


Figure 2: Photographs of the experimental slopes (a: Mizuno-no-Sawa in 2016−18, b: Moiwa Bowl in 2019, c: Mizuno-no-Sawa in 2025).

was concluded without performing experiments in 2020 due to restrictions on travel imposed by the COVID-19 pandemic. In 2025, the experiment was resumed using different, short-term project funding. This was done on the suggestion of a ski resort staff that it might be more successful to observe avalanches during avalanche control operations in the severe winter season.

We employed the following instrumentation (Tables 1 and 2):

Drone. Observation of avalanche movement and surveys of slope topography and avalanche size based on pre- and post-experiment changes in the snow surface (DJI Phantom 4 was/were used throughout all the experiments, a DJI Matrice 300 RTK with Zenmuse L1 LiDAR module was also used in 2025).

Doppler radar. Measurements of avalanche velocity spectra (Schreiber et al., 2001).

Inertial Measurement Unit (IMU) and Global Navigation Satellite System (GNSS). Released within the avalanche flow to measure the internal velocity (Neuhauser et al., 2025) (in 2017−19, Sports Sensing SS-WSD1201 was used, replaced by AvaNodes in 2025).

Measurement wall. A wall aligned parallel to the flow was installed on the slope, equipped with nine pairs of LED and photodiode sensors at different heights, to determine the vertical profile of down-slope velocity and its fluctuations within the avalanche (Dent et al., 1998). A load cell and a pore-air pressure sensor were also installed next to each other to determine the effective normal stress of the avalanche (Issler and Ito, 2024).

Seismic and infrasound sensors. Detection or tracking of the flow from induced ground vibrations and generated infrasound (Pérez-Guillén et al., 2019; Johnson et al., 2021). (In 2016−18 and in 2025, Sercel (Mark Products) L-22D-3D seismometer(s) and Paroscientific 6000-16B infrasound sensor(s) was used; in addition, Lennartz LE-3D MkII/MkIII seismometers were used in 2018 and 2019).

Infrared camera. Observation of changes in snowpack temperature associated with avalanche flow (Steinkogler et al., 2014) (a FLIR C2 was used in 2017, an Avio InfREC R300SR was used in 2018 and 2019, a DJI Zenmuse H20T camera module was used in 2025).

LiDAR. Measuring the flow thickness of the dense avalanche flow (a Livox AVIA was used).

Table 1: Overview of equipment used in 2016 and 2017.

Year	***Exp.1 (2016)***	***Exp.2 (2017)***
Drone	1	1 (Mizuno-no-sawa only)
Doppler radar	–	–
IMU and GNSS	–	3
Measurement wall	–	–
Seismic sensor	1	1
Infrasound sensor	1	1
Infrared camera	–	1
LiDAR	–	–

Table 2: Overview of equipment used in 2018, 2019, and 2025.

Year	***Exp.3 (2018)***	***Exp.4 (2019)***	***Exp.5 (2025)***
Drone	3	3	2
Doppler radar	1	1	1
IMU and GNSS	5	2	3
Measurement wall	1	–	1
Seismic sensor	6	3	1
Infrasound sensor	3	–	1
Infrared camera	1	1	1
LiDAR	–	–	1

3. RESULTS

3.1 Overview of experiments

The following provides an overview of the SAEs conducted between 2016 and 2019, and in 2025.

Exp.1 (Winter 2016). The first experiment in Niseko took place at Mizuno-no-Sawa on 28 March. The main objective was to verify whether it was possible to trigger wet-snow avalanches by blasting. The observation equipment was limited to a minimum. The experiment succeeded in triggering an avalanche using the explosive charge.

Exp.2 (Winter 2017). On 17 March, an experiment using a snow groomer was carried out at Moiwa Bowl. The main objective was to verify whether IMU sensors would travel within the avalanche. Of the two attempts, one successfully triggered an avalanche, confirming that the IMU sensors travelled within it. On 25 March, an avalanche was successfully triggered by explosives at Mizuno-no-Sawa. Two of the three IMU sensors placed near the blast site were swept along by the avalanche.

Exp.3 (Winter 2018). On 23 March, measurement equipment was set up at Mizuno-no-Sawa, but no avalanche was triggered despite repeated use of

explosives. This is likely because snowmelt during the day had softened the bonding between snow particles, causing rapid dissipation of the explosion pressure inside the soft snowpack.

Exp.4 (Winter 2019). We had planned to conduct an experiment at Mizuno-no-Sawa as in 2018. However, this became impossible due to the risk of spontaneously releasing or human-induced avalanches as the entire snowpack had become unstable by rapid snowmelt. Consequently, we decided to carry out the experiment at Moiwa Bowl on 25 March. As the snowpack consisted of decomposed precipitation particles containing a weak layer overlying a melt-freeze crust, a small avalanche was successfully triggered using a snow groomer.

Exp.5 (Winter 2025). We observed snow avalanches triggered during avalanche control operations commencing from 7 AM on 30 January. After a long period with little snowfall, fresh snow accumulated on a melt-freeze crust from the day before the experiment, causing several very small avalanches to be triggered by the blasting. Unlike in other years, this was conducted in January during high winter, resulting in dry snow avalanches.

3.2 Experimental Results

Avalanche size. The runout distance and debris volume of avalanches were determined from drone surveys conducted before and after the avalanche release. The largest example was the avalanche in the Exp.1 (2016), which had a runout distance of approximately 210 m and a debris volume of approximately 520 m³. Conversely, the smallest example was the avalanche in the Exp.5 (2025), four small avalanches with runout distances ranging from approximately 30 to 50 m were triggered simultaneously from multiple locations by blasting. However, due to time constraints, the survey immediately prior to the experiment could not be carried out, hence the volume of the debris could not be determined. Another example of a smaller case was found in the Exp.4 (2019); an avalanche triggered by a snow groomer had a runout distance of approximately 40 m and a debris volume of approximately 25 m³.

While changes in width of the flowing avalanche can be determined from airborne drone footage, it is difficult to accurately measure changes in thickness. In the Exp.5 (2025), an attempt was made to measure changes in thickness during flow using LiDAR. However, no data was obtained during the experiment because the battery ran out. In the data recorded before the experiment, reflections from snowflakes in the air made it difficult to clearly obtain the snow surface in the signal.

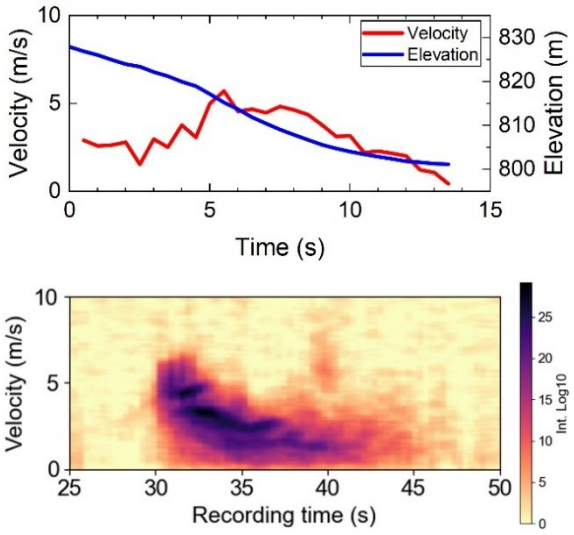


Figure 3: Avalanche velocity measured in the Exp.4 (2019). Top: Leading-edge velocity obtained from drone aerial footage; Bottom: Velocity spectra obtained from Doppler radar at 197−213 m range gate.

Velocity. The avalanche velocity was determined using four methods: 1. Changes in the position of the leading edge obtained from aerial drone footage. 2. Velocity spectra from Doppler radar. 3. Position data from a sensor containing a GNSS receiver travelling down within the avalanche. 4. The time difference in signals and the distance between the pair of optical sensors mounted on the measurement wall. The highest velocity recorded in past experiments was over 10 m/s during a relatively large avalanche in the Exp.1 (2016). In the Exp.4 (2019), experiments were conducted using methods 1−3 simultaneously. The velocity measurements obtained from the drone and the Doppler radar showed good agreement (Fig. 3), while the GNSS failed to record the position. Although this avalanche was rather smaller in scale, with a runout distance of 40 m, significant results were obtained even with a Doppler radar having a range gate of 15 m. In the Exp.5 (2025), experiments were conducted using all four methods. However, the Doppler radar failed to start up; and the measurement wall equipped with optical sensors did not obtain sufficient data, as battery-saving timer settings resulted in it ceasing operation before the experiment began. The other velocity measurements obtained using the drone and GNSS showed relatively good agreement (Fig. 4). Note that, due to the shallow extent of the avalanche flow, the sensor equipped with GNSS bounced upon the hard snow surface at the early stage of motion, occasionally yielding larger values than the actual avalanche velocity (see the velocity peak around 22:28:30 UTC in the bottom panel of Fig. 4).

Flow behavior. Infrared camera imaging was carried out to observe the flowing behavior of avalanches. Figure 5 was captured during the Exp.4 (2019). The piled-up snow, pushed and collapsed by a snow groomer, plowed the warm surface layer (the red area in Figure 5), exposing the cold snow beneath. While such movement of a dense core is rarely observable in large-scale avalanches, as it is obscured by the powder snow cloud, it is clearly visible in small avalanches. As the runout distance was short, no dynamic mixing was observed.

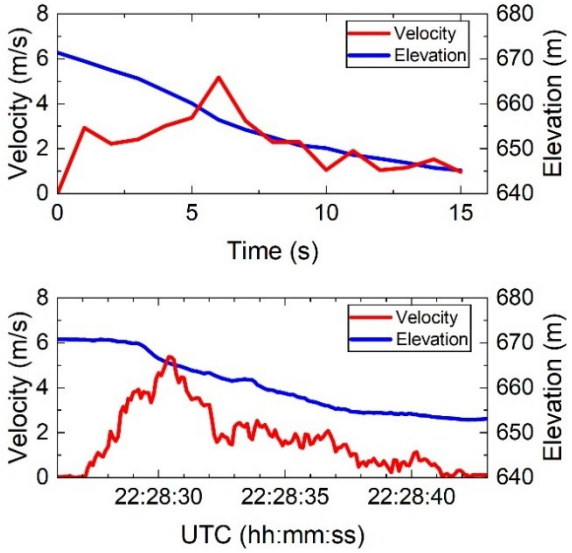


Figure 4: Avalanche velocity measured in the Exp.5 (2025). Top: Leading-edge velocity obtained from drone aerial footage; Bottom: Internal velocity obtained from GNSS data.

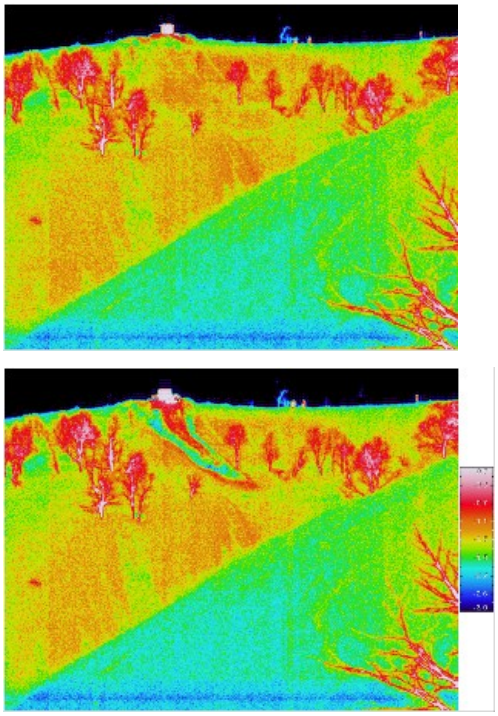


Figure 5: Infrared images before (top) and after (bottom) the avalanche in the Exp.4 (2019). Note the warm snow near the middle line of the flow path and at the tip of the deposit. Cold snow is found behind the front and along the edges of the deposit.

By staining cross-sections and/or longitudinal sections of the debris with ink after the avalanche has stopped (a method pioneered by Gubler in the 1980s, see Issler et al., 2008), it is often possible to distinguish the undisturbed part of the snow cover from the overlying debris and to visualize the granulometry of the deposit. This can give crucial information on the flowing processes including the entrainment of the snow cover. Figure 6 shows an example of debris after the Exp.5 (2025). In this case, as only a thin layer of fresh dry snow flowed down on a hard snow crust, no entrainment and formation of snow blocks could be observed.

Seismic and infrasound signals. As the small avalanches in the Exp.2 (2017) flowed down, ground motion could be measured at a distance of around 100 m, while no clear infrasound signals were obtained (Fig. 7). This suggests that the small surfaces, short acceleration periods and low velocities of small avalanches produce insufficient displacement of the surrounding air relative to the natural background noises. Moreover, it has been found that releasing avalanches using snow groomers is unsuitable for measuring seismic signals, as the noise generated by the groomer's movement is significantly greater than the signals.

Velocity profiles and pressure. Unfortunately, no data has been obtained from the measurement wall so far: It was not designed and built yet in 2016 and 2017; in 2018 no avalanche could be released, in 2019 it was not installed in the slope due to time constraints, and in 2025 the data could not be obtained due to a problem with a battery-saving timer.



Figure 6: Coloration of debris (left) and longitudinal-section of the debris (right) in the Exp.5 (2025).

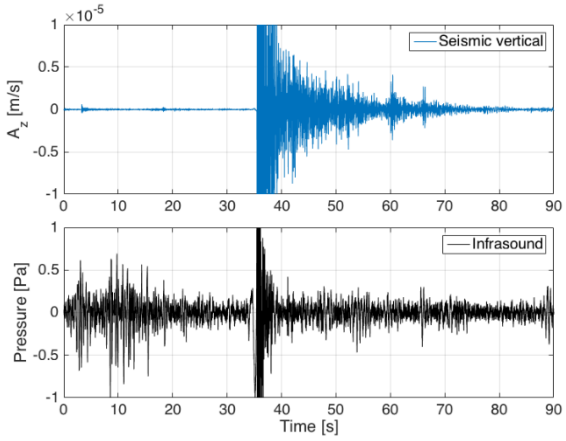


Figure 7: Seismic (top) and infrasound (bottom) signals in the Exp.2 (2017). The waveform prior to 40 s was caused by an explosion.

4. DISCUSSION AND OUTLOOK

The dynamics of small avalanches has been observed using various methods. However, some important parameters, such as impact pressure, that have yet to be measured. Furthermore, there has not yet been a successful case where all expected measurements were achieved. This is due to the significant constraints involved in conducting experiments at ski resorts. For one, the experimental schedule is heavily dependent on the availability of ski resort staff and limited to early mornings or late afternoons, leaving insufficient time for post-event field work. Another severe limitation is that, as skiers and snowboarders use the experimental slope, it is difficult to install permanent experimental equipment due to the risk of accidents caused by collisions. Consequently, it is necessary to set up the equipment immediately prior to the experiment, which has frequently led to problems arising from inadequate preparation. Furthermore, due to the deep snow cover at Niseko, sensors in the slope, like the measurement wall, must be embedded or anchored in the snow rather than the ground; consequently, if the impact force of an avalanche is greater than anticipated, the sensors may be destroyed or swept away.

On the other hand,experiments at ski resorts have the advantage that avalanches can be triggered using explosives and snow groomers, which researchers are not usually allowed to handle. Additionally, there are open slopes suitable for experiments, and personnel and experimental equipment can be easily transported using ski lifts and snow groomers. Even if an ideal slope exists outside a ski resort, it requires researchers to trigger an avalanche themselves. While there are ideas for methods to trigger small avalanches without explosives and snow groomer (Issler and Ito, 2024), these have not been sufficiently verified; therefore, it is necessary to conduct avalanche-triggering tests as a preliminary step to the experiment.

Another advantage is that the absence of permanent experimental equipment can provide an incentive to introduce new observational methods. For example, equipment such as LiDAR, employed to measure the thickness of the flow, would likely be difficult to utilize in large-scale avalanche experiments. Thus, SAEs are well-suited as a field for testing new and innovative sensing technologies. In addition to sensing, the possibility of observing flow behaviour and avalanche deposits at close range contributes to a deeper understanding of avalanche dynamics.

To conduct the experiments, we utilized short-term research project funding. This enabled us to bring together a large number of researchers and a wide range of equipment for the experiments. However, the large number of participants also led to scheduling problems and experiments being conducted under unsuitable conditions (e.g. little snowfall, excessively high temperatures). In order to maintain a sustainable system for SAEs, it is necessary to continue the experiments by carefully selecting parameters that can be measured even with a small team and low budget while still providing highly relevant data for understanding the properties of small avalanches and testing and improving numerical models and mitigation measures. As a first step in this direction, we plan to reanalyze the data collected so far and to test existing avalanche models against them.

ACKNOWLEDGEMENTS

We would like to express our gratitude to Mr. Eiichi Tanaka, Mr. Nobuyuki Nomura, Mr. Hideki Yokoo and Mr. Futa Takeda of Niseko Village Ski Resort, and to Mr. Masaya Yoshimura, Mr. Kazuto Oba and Mr. Ryuji Omichi of Niseko Moiwa Ski Resort, as well as the many other ski resort staff members who provided invaluable assistance with the avalanche experiments.

This work was partly supported by JSPS KAKENHI (grant nos. JP15H02992 and JP21H04601) and by the Research Council of Norway and the Directorate for Higher Education and Skills (project Climate-Induced Geohazards Mitigation, Management, and Education in Japan, South Korea, and Norway (GEOMME), grant no. 322469).

REFERENCES

Abe, O., Sato, A., Nohguchi, Y., Nakamura, T., Qiu, J., Xu, J., Jiang, F., and Wang, X., 1999. Study on the dynamics of an artificial avalanche in the Tianshan Mountains, China, Rep. Natl. Res. Inst. Earth Sci. Dis. Prevention, 59, 19−30, doi:10.24732/nied.00001099 (in Japanese with English abstract).

Barbero, M., Barpi, F., Borri-Brunetto, M., Bovet, E., Chiaia, B., Biagi, V. D., Frigo, B., Pallara, O., Maggioni, M., Freppaz, M., Ceaglio, E., Godone, D., Viglietti, D., and Zanini, E. 2013. A new experimental snow avalanche test site at Seehore peak in Aosta Valley (NW Italian Alps) − Part II: Engineering aspects, Cold Regions Sci. Technol., 86, 14−21, doi:10.1016/j.coldregions.2012.10.014.

Christen, M., Bartelt, P., Kowalski, J., 2010. Back calculation of the In den Arelen avalanche with RAMMS: interpretation of model results. Ann. Glaciol., 51(54), 161−168, doi:10.3189/172756410791386553.

Dent, J. D., Burrell, K. J., Schmidt, D. S., Louge, M. Y., Adams, E. E., and Jazbutis, T. G., 1998. Density, velocity and friction measurements in a dry-snow avalanche. Ann. Glaciol., 26, 247−252, doi:10.3189/1998AoG26-1-247252.

Gauer, P. and Kristensen, K., 2016. Four decades of observations from NGI's full-scale avalanche test site Ryggfonn −Summary of experimental results. Cold Regions Sci. Technol., 125, 162−176, doi:10.1016/j.coldregions.2016.02.009, 2016.

Issler, D., Errera, A., Priano, S, Gubler, H., Teufen, B. and Krummenacher, B., 2008. Inferences on flow mechanisms from snow avalanche deposits, Ann. Glaciol. 49(1), 187−192, doi:10.3189/172756408787814915.

Issler, D. and Ito, Y., 2024. Thoughts on the why's and how's of small-avalanche experiments. *In:* Proc. International Snow Science Workshop 2024, Tromsø, 393−400, https://arc.lib.montana.edu/snow-science/objects/issw2024_P2.14.pdf.

Johnson, J. B., Anderson, J. F., Marshall, H. P., Havens, S., and Watson, L. M., 2021. Snow avalanche detection and source constraints made using a networked array of infrasound sensors. Journal of Geophysical Research: Earth Surface, 126, e2020JF005741, doi:10.1029/2020JF005741.

Kern, M. A., Tiefenbacher, F., and McElwaine, J. N., 2004. The rheology of snow in large chute flows. Cold Regions Sci. Technol., 39(2−3), 181−192, doi:10.1016/j.coldregions.2004.03.006.

Maggioni, M., Freppaz, M., Christen, M., Bartelt, P., and Zanini, E., 2012. Back-calculation of small avalanches with the 2D avalanche dynamics model RAMMS: Four events artificially triggered at the Seehore test site in Aosta Valley (NW Italy). *In:* Proc. International Snow Science Workshop 2012, Alaska, 591−598, https://www.academia.edu/download/91331979/issw-2012-591-598.pdf.

Maggioni, M., Barbero, M., Barpi, F., Borri-Brunetto, M., De Biagi, V., Freppaz, M., Frigo, B., Pallara, O., and Chiaia, B., 2019. Snow avalanche impact measurements at the Seehore test aite in Aosta Valley (NW Italian Alps), Geosci., 9, 471, doi:10.3390/ geosciences9110471.

Neuhauser, M., Köhler, A., Neurauter, R., Adams, M. S., and Fischer, J. T., 2025. Particle trajectories, velocities, accelerations and rotation rates in snow avalanches. Ann. Glaciol., 65, e9, doi:10.1017/aog.2023.69.

Nishimura, K., Pérez-Guillén, C., Ito, Y., Yamaguchi, S., Saito, Y., Issler, D., and Fischer, J. T., 2018. Studies on snow avalanche dynamics by full-scale experiments. *In:* Proc. International Snow Science Workshop 2018, Innsbruck, 50−53, http://arc.lib.montana.edu/snow-science/objects/ISSW2018_P01.8.pdf.

Pérez-Guillén, C., Tsunematsu, K., Nishimura, K., and Issler, D., 2019. Seismic location and tracking of snow avalanches and slush flows on Mt. Fuji, Japan. Earth Surface Dynamics, 7(4), 989−1007, https://doi.org/10.5194/esurf-7-989-2019.

Schaefer, M., 2016. Shear and normal stresses measured on the Weissfluhjoch Snow Chute. Canadian Geotechnical Journal. 53(3), 445−454, doi:10.1139/cgj-2015-0211.

Schreiber, H., Randeu, W. L., Schaffhauser, H., Rammmer, L., 2001. Avalanche dynamics measurement by pulsed Doppler radar. Ann. Glaciol., 32,275−280, doi:10.3189/172756401781819021.

Sommavilla, F., and Sovilla, B., 1988. The avalanche monitoring system of Mount Pizzac, *In:* 25 Years of Snow Avalanche Research, Voss, 1998, ed. Hestnes, E., Publication Nr. 203, 268−273, Norwegian Geotechnical Institute, Oslo, Norway.

Sovilla, B., McElwaine, J., Steinkogler, W., Hiller, M., Dufour, F., Suriñach, E., Baroudi, D., 2013. The full-scale avalanche dynamics test site Vallée de la Sionne. *In:* Proc. International Snow Science Workshop 2013, Grenoble−Chamonix Mont-Blanc, 1350−1357, https://arc.lib.montana.edu/snow-science/objects/ISSW13_paper_O4-33.pdf.

Steinkogler, W., Sovilla, B., and Lehning, M., 2014. Linking snow cover properties and avalanche dynamics. *In:* Proc. International Snow Science Workshop 2014, Banff, 151−155, https://www.academia.edu/download/74567436/ISSW14_paper_O6.04.pdf.

Vilajosana, I., Llosa, J., Schaefer, M., Surinach, E., and Vilajosana, X., 2011. Wireless sensors as a tool to explore avalanche internal dynamics: Experiments at the Weissflühjoch Snow Chute. Cold regions sci. technol., 65(2), 242−250, doi:10.1016/j.coldregions.2010.09.011.